Chemical Science

EDGE ARTICLE

View Article Online
View Journal | View Issue

Cite this: *Chem. Sci.*, 2015, **6**, 4828

Synthesis of triazolium-based mono- and tris-branched [1]rotaxanes using a molecular transporter of dibenzo-24-crown-8†

P. Waelès, C. Clavel, K. Fournel-Marotte and F. Coutrot*

Received 11th May 2015
Accepted 28th May 2015

DOI: 10.1039/c5sc01722j

www.rsc.org/chemicalscience

We report a diverted route to [1]rotaxane and tris-branched [1]rotaxane that are devoid of any efficient template and which could not be obtained by classical straightforward strategies. The described chemical route relies on the utilization of a "macrocycle transporter", which is able first to bind a macrocycle, second to link temporarily a triazolium-containing molecular axle, and third to deliver the macrocycle around the new docked axle through molecular machinery in a [1]rotaxane structure. The extended encircled thread is eventually cleaved by an amine or a triamine to afford the triazolium-containing [1]rotaxanes, releasing at the same time, the macrocycle transporter as a recyclable species.

Introduction

Since the properties of molecules are closely related to their tridimensional structure, mechanically interlocked molecules,[1] which adopt very unusual and interesting architectures, seem to be very appealing potential targets in a wide range of research fields. It follows that improving their chemical access is of the highest interest, even though it might be a challenging task in some cases. Among the numerous interlocked molecular architectures, the [1]rotaxane[2] molecular architecture holds a unique position, being a single molecule. It consists of a macrocycle that surrounds a molecular thread, in which both components are connected together through a covalent bond. Several different chemical routes have been used to synthesize [1]rotaxanes up to now (Fig. 1). The least used strategy relies on a covalent bond formation and was reported by Hiratani *et al.* in 2004 (synthetic pathway (a)):[3] in that case a key bicyclic intermediate is statistically attacked either by the inner region of the macrocycle to afford the [1]rotaxane, or by the outside of the macrocycle to provide the non-interlocked analogue. More frequently encountered are the other strategies relying on the use of weak interactions as the driving force to assemble the molecular elements into the self-interlocked architecture. They can be divided into three main synthetic pathways. The first one relies on the preliminary template-directed synthesis of a semi [2]rotaxane followed by the chemical connection between the surrounded axle and the macrocycle (synthetic pathway (b)).[4] The second one uses a "hermaphrodite" molecule, that is to say a macrocycle that is covalently bonded to a molecular axle which contains a site of interaction for the macrocycle (synthetic pathway (c)). In that case, the non-interlocked molecule remains in equilibrium with the pseudo[1]rotaxane, until the latter is capped either by a hindering[5] or a rigid stopper[6] at the extremity of the axle. The third templated pathway consists in a self-entanglement strategy of a "hermaphrodite" molecule that already contains a stopper at the extremity of the axle (synthetic pathway (d)). In that particular case, no threading of the bulky extremity is allowed, so that the only way to interlace the molecule is to perform a pirouette of one part of the macrocycle (*i.e.* the section connected to the axle) with respect to the other.[7] This last templated strategy is probably a more demanding chemical pathway to set up since it requires a macrocycle of a bigger cavity to allow the self-entanglement, although enough interactions must be maintained at the same time between the template and the macrocycle to obtain the [1]rotaxane structure. Herein, we report on the synthesis of triazolium-containing mono- and tris-branched [1]rotaxanes which are devoid of any efficient template for the macrocycle (Fig. 2). They only contain a triazolium moiety which serves as a molecular station of poor affinity for the dibenzo-24-crown-8 (DB24C8) derivative in a locked rotaxane.

The newly proposed synthetic strategy relies on the use of a recyclable transporter of macrocycles, **A**, whose utility is to catch a macrocycle and to deliver it to another axle (Fig. 3).[8] As it has been designed to contain an efficient template moiety for the macrocycle, **A** initially efficiently captures the

Supramolecular Machines and Architectures Team, Faculté des Sciences, Institut des Biomolécules Max Mousseron (IBMM) UMR 5247 CNRS, Université Montpellier, ENSCM, case courrier 1706, Bâtiment Chimie (17), 3ème étage, Place Eugène Bataillon, 34095 Montpellier cedex 5, France. E-mail: frederic.coutrot@univ-montp2.fr; Web: http://www.glycorotaxane.fr; Fax: +33 4 67 63 10 46; Tel: +33 4 67 14 38 43

† Electronic supplementary information (ESI) available: Full experimental procedures and characterization data for all compounds. See DOI: 10.1039/c5sc01722j

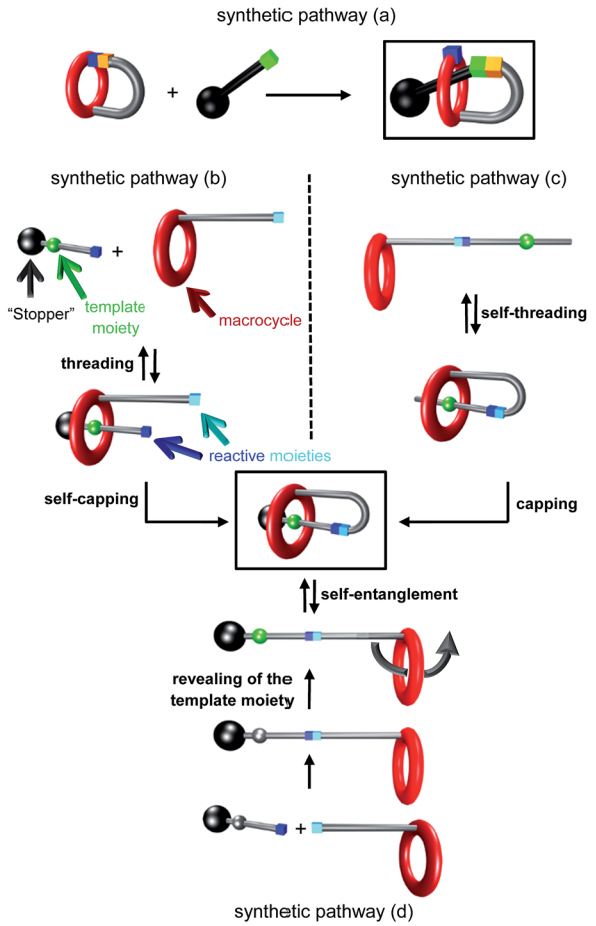

Fig. 1 Chemical templated routes to [1]rotaxanes.

macrocycle so forming the semi[2]rotaxane **B** in a similar fashion as in the illustrated strategy (b) of Fig. 1. Extension of the encircled axle, then self-capping through the linking between the thread end and the substituted macrocycle provides the locked [1]rotaxane structure **D**. At this step, a second site of interaction of much poorer affinity for the macrocycle is also created in the encircled axle. Molecular machinery is subsequently used to trigger the tightening of the [1]rotaxane lasso **D**, through the shuttling of the macrocycle around the final targeted axle. The final step of the strategy consists in the cleavage of the axle of the tightened [1]rotaxane **E** using a functionalized stopper, thus providing simultaneously the contracted [1]rotaxane **F** and the initial modified axle **G**. Eventually, the initial transporter **A** can be regenerated through the recycling of **G**. What is here very important to point out is the effectiveness of the strategy. Indeed, the final triazolium-containing[1]rotaxane **F** (*i.e.* **6** and **7**) cannot be efficiently generated using the other already reported strategies. Although the second created site of interaction for the macrocycle (*i.e.* triazolium) acts as an effective molecular station for the shuttling of the macrocycle in the locked [1]rotaxane structure, it would not permit to drive the rotaxane formation through intermolecular interactions, this being mainly due to entropic factors.[9]

Results and discussion

Preparation of the loosened extended [1]rotaxane D

The synthetic sequence begins by the slippage[10] of a transporter of macrocycle **1** (Scheme 1). It contains an ammonium moiety (in green) which initially serves as an efficient template for the DB24C8.[11] It also contains a *tert*-butylbenzyl stopper (in black) at one extremity and a *N*-hydroxysuccinimide (NHS) moiety (in blue) at the other end. The semirotaxane architecture **2** could be obtained in 83% yield after stirring during 12 h in dichloromethane at room temperature, 3 equivalents of the DB24C8 derivative and 1 equivalent of **1** at a concentration of 0.12 M. The bulkiness of the NHS is responsible for the long slippage process and for the stability of the product. Indeed, it is noteworthy that the rotaxane **2** is stable as a powder and can be kept for many days without observing any disassembly. Furthermore, the unthreading is also very slow in a hydrogen-bond promoting solvent such as dichloromethane, which is beneficial here since it allows the purification of **2** by Sephadex chromatography. The extension of the encircled axle was then carried out by esterification of the free hydroxyl group of the NHS-containing rotaxane **2** with the azido hexanoic acid, using dicyclohexylcarbodiimide as coupling reagent. On the one hand, it provides a *N*-hydroxysuccinimide ester moiety, which will be of utility for the final cleavage step of the strategy. On the other hand, the incorporated azido moiety (in purple), gives the opportunity to self-cap the [1]rotaxane architecture through cyclization. The azido moiety of the extended [2]rotaxane **3** was therefore connected to the alkyne-containing macrocycle, through copper(I)-catalyzed Huisgen[12] alkyne-azide 1,3-dipolar cycloaddition.[13] High dilution (5×10^{-4} M) conditions were employed to provide the [1]rotaxane architecture in a satisfactory yield of 60%. The so-created triazole moiety was further methylated before being submitted to an anion exchange using ammonium hexafluorophosphate, affording **4l** with an overall yield of 54% from **3**. This alkylation reveals the *N*-methyltriazolium in **4** as the second site of interaction for the DB24C8 derivative.[14] In hydrogen-bond promoting solvents, as long as the ammonium remains protonated, the DB24C8 derivative is mainly localized around the more favorable ammonium station, resulting in a loosened conformation of the lasso. Since the chemical route to the targeted [1]rotaxanes **6** and **7** requires the large-amplitude shuttling of the macrocycle along the thread toward the triazolium station, the displacement of the equilibrium from the loosened lasso **4l** to the tightened lasso **4t** was envisaged. We first studied the effect of a variation of the polarity of the medium. Through a more efficient subsequent approach, an *N*-carbamoylation of the ammonium station was then considered.

Tightening of the lasso through solvent-dependent molecular machinery

The partial tightening of the loosened lasso **4l** was found to be possible through molecular machinery, upon variation in solvent polarity (Scheme 1). In acetonitrile, the DB24C8 derivative resides exclusively around the ammonium station, affording the loosened conformation for the lasso **4l**. This was

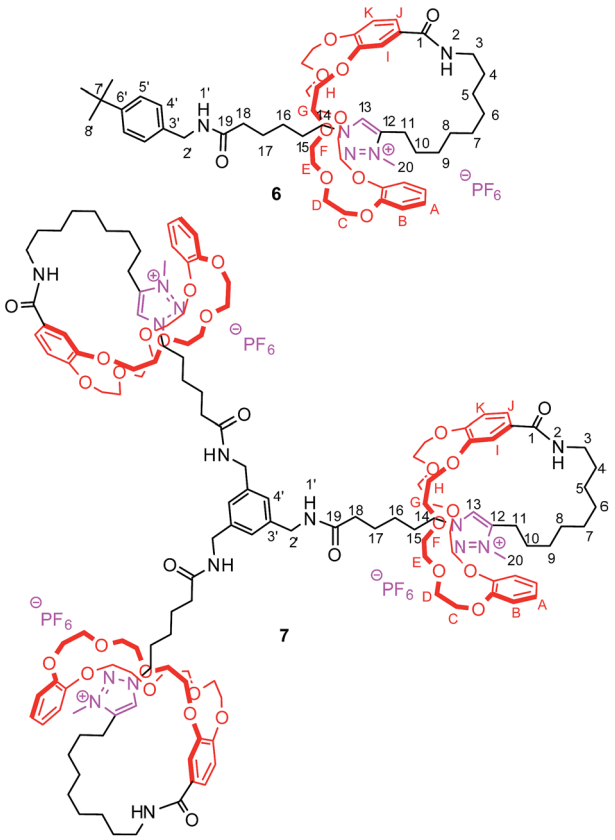

Fig. 2 Synthesized [1]rotaxanes **6** and **7** with atom assignments.

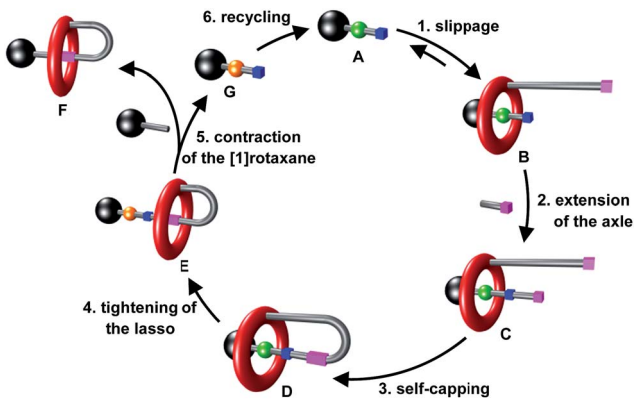

Fig. 3 A novel route to [1]rotaxane **F** based on a recyclable macrocycle transporter **A**.

demonstrated by the direct comparison between the ^{1}H NMR spectra of the [1]rotaxane **4l** and its non-interlocked analogue **4u** (Fig. 4a–b). First of all, only one set of ^{1}H NMR signals can be observed in **4l**, which indicates the presence of the DB24C8 only around one of the two stations.[15] Moreover, no significant variation of the chemical shifts is observed for the hydrogen atoms ($H_{11,13,14,20}$) of the triazolium moiety of lasso **4l** and the non-interlocked analogue **4u**. On the contrary, the hydrogen atoms belonging to the ammonium station, *i.e.* $H_{15'}$ and in a lesser extent $H_{13'}$, are both shifted downfield in **4l** ($\Delta\delta$ = 0.42 and 0.13 ppm, respectively), due to their hydrogen-bonding interactions with the oxygen atoms of the DB24C8. At the same time, hydrogens $H_{8'-12'}$ are all more or less shielded in **4l** (from −0.54 to −0.25 ppm) because of their localization in the shielding cavity of the aromatic rings of the DB24C8. Concerning the methylene hydrogens H_{C-H} of the DB24C8 part, they are all split in the interlocked lasso **4l**, because they are facing the two non-symmetrical ends of the threaded axle. Besides, we note the upfield shift undergone by hydrogens H_{E-F} in **4l**, due to their localization in the shielding cavity of the benzyl ammonium aromatic ring of the encircled axle, therefore corroborating the localization of the DB24C8 around the ammonium station in acetonitrile. In DMSO, the behaviour of the lasso **4** appeared slightly different (Fig. 4c–e).

Indeed, although the exclusive loosened conformation **4l** was observed in DMSO at $t = 0$ (Fig. 4d and e),[16] the appearance of a second set of ^{1}H signals was noted with time. This corresponds to the tightened conformation of the lasso (**4t**). After 22 h, the equilibrium between the two translational conformers was reached and a ratio **4l** : **4t** of about 80 : 20 was observed (Fig. 4c). This ratio remained unchanged either upon longer time or by heating the sample. Without any doubt, the new set of signals matches with the tightened conformation **4t**, in which the DB24C8 is localized around the triazolium station. This is quite a surprising result, taking into account the much better affinity of the DB24C8 for the ammonium station than for the triazolium. One may suggest that the solvation effect of the DMSO is stronger on the ammonium than on the triazolium, therefore decreasing the difference of affinity between the two respective stations for the DB24C8, hence triggering the slight displacement of the equilibrium toward the tightened lasso **4t**. The tightening of the lasso **4** in DMSO was evidenced by the direct comparison between the ^{1}H NMR spectra of the lasso **4t** and the non-interlocked analogue **4u** (Fig. 4c and e). To summarize, in DMSO-d_6 the new set of signals matches with **4t**: indeed, the chemical shifts of the hydrogen atoms belonging to the triazolium site (*i.e.* $H_{11,13,14,15,20}$) are all affected by the new localization of the DB24C8. In **4t**, it is noteworthy to point out both the deshielding and the splitting of H_{14} ($\Delta\delta$ = 0.37 and 0.5 ppm), the downfield shift of H_{15} ($\Delta\delta$ = 0.37 ppm), and the shielding of H_{11}, H_{13} and H_{20} ($\Delta\delta$ from −0.44 to −1.16 ppm).[17] Meanwhile, no variations at all of chemical shifts are noticed between **4t** and **4u** for the hydrogen atoms $H_{13',14',15'}$ that belong to the ammonium station, which is in accordance with the tightened conformation. Although a partial tightening of the lasso **4** was possible in the more polar solvent DMSO, the obtained ratio (20%) was not found sufficient to efficiently pursue the synthesis of the triazolium-based [1]rotaxanes **6** and **7**. We thus decided to use a chemical stimulus to generate the tightened lasso in high yield through the actuation of the molecular machinery.

Tightening of the lasso by molecular machinery through the *N*-carbamoylation of the ammonium

In a second approach, the *N*-carbamoylation of the ammonium was carried out in order to displace quantitatively the DB24C8

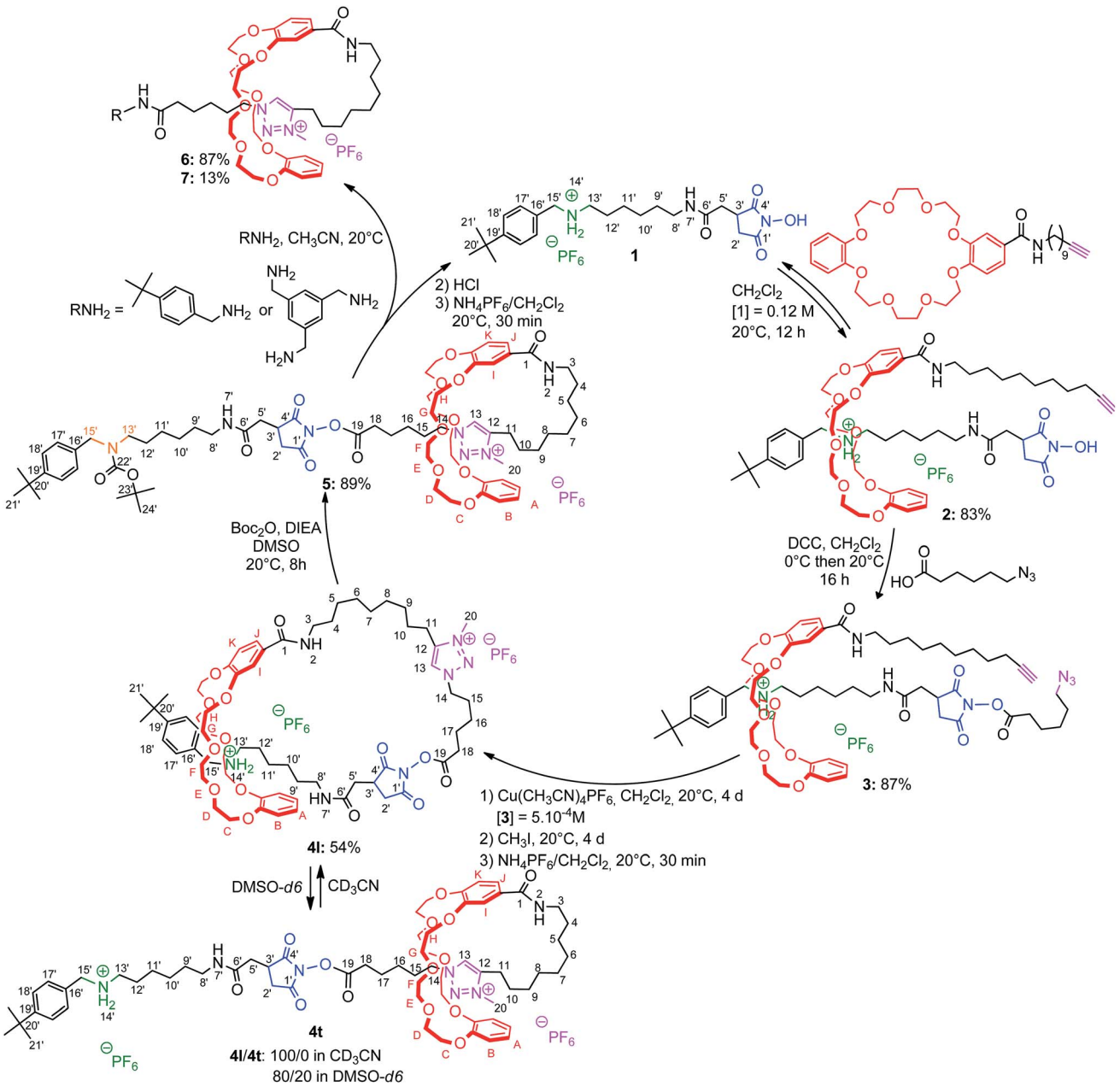

Scheme 1 Preparation of mono- and tris-branched triazolium-containing [1]rotaxanes using the recyclable macrocycle transporter **1**.

around the triazolium station. Similarly to the *N*-acetylation,[18] the *N*-carbamoylation[19] of a complex ammonium/DB24C8 was reported as a demanding task in acetonitrile because of the strong hydrogen-bonding interactions between the components. This results in the decrease of the acidity of the ammonium, therefore dramatically diminishing the kinetics of the overall reaction. In a previous paper, we improved the *N*-carbamoylation by using a strong base such as phosphazene, although some side-products resulted from the harsher conditions.[8] Here, the *N*-carbamoylation was successfully achieved without any side-reaction with the help of the weak base diisopropylethylamine and Boc_2O, however this is in the more polar solvent DMSO. The DMSO was effectively chosen because its high polarity decreases the binding affinity of the ammonium for the crown ether, hence increasing its acidity and facilitating its deprotonation in very mild conditions. The tightened carbamoylated lasso **5** could be obtained and isolated this way in 89% yield.[20] The localization of the crown ether around the triazolium was established by comparing the ^{1}H NMR spectra of the respective loosened and tightened lassos **4l** and **5** with their respective non-interlocked analogue **4u** and **5u** (Fig. 5).

As already discussed in the preceding section, the comparison between the ^{1}H NMR spectra of **4u** and **4l** demonstrated the localization of the crown ether around the ammonium station in **4l** (Fig. 5a and b). After carbamoylation, the crown ether

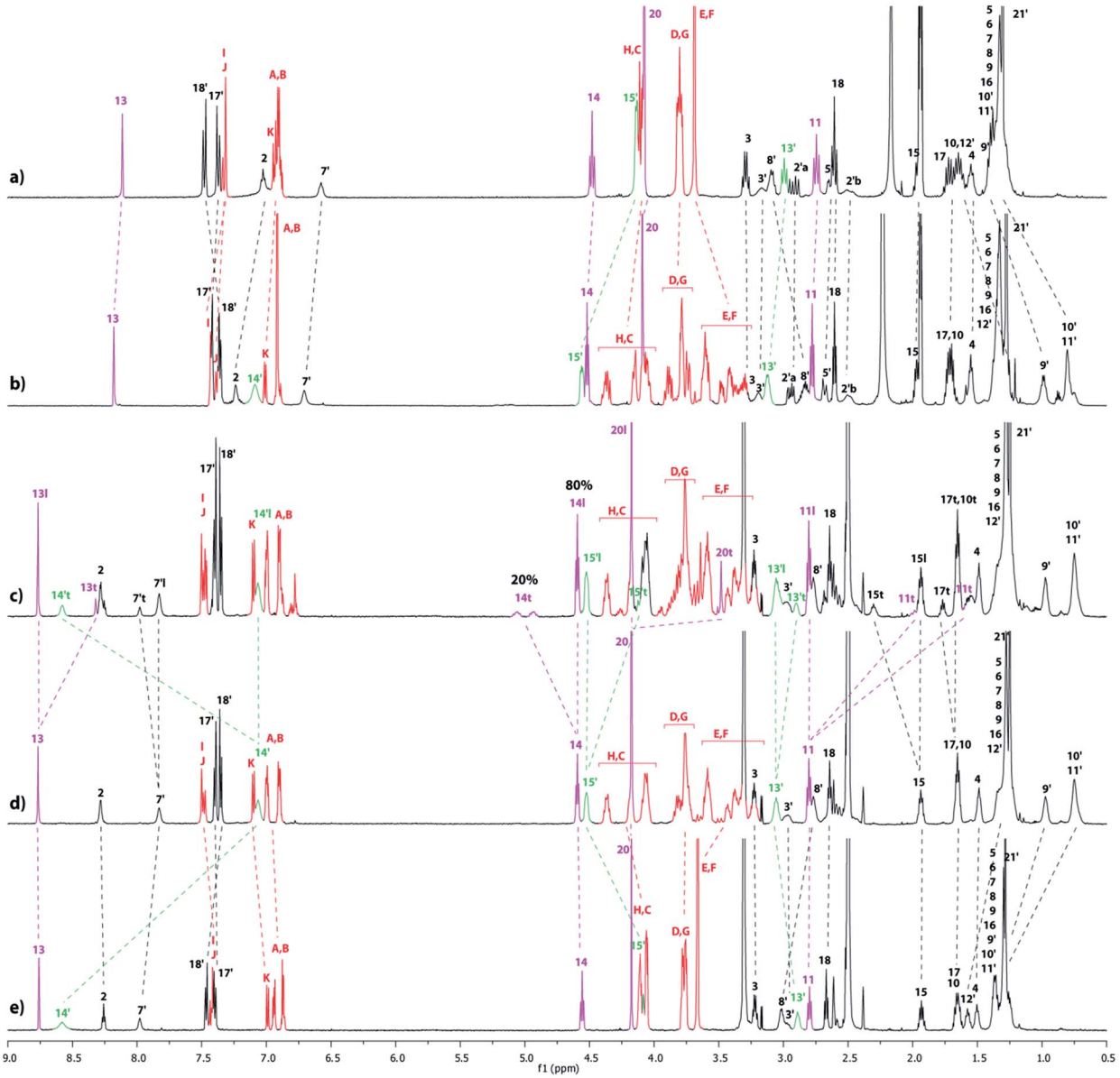

Fig. 4 ^{1}H NMR Spectra (600 MHz, 298 K) of (a) the non-interlocked analogue **4u** in CD_3CN, (b) the loosened [1]rotaxane **4l** in CD_3CN, (c) the loosened and tightened [1]rotaxanes **4l** and **4t** in DMSO-d_6 at $t = 20$ h, (d) the [1]rotaxane **4l** in DMSO-d_6 at $t = 0$ h and (e) the non-interlocked analogue **4u** in DMSO-d_6. The numbering and colorings correspond to the hydrogen assignments indicated in Scheme 1.

glides around the triazolium station, resulting in the tightening of the lasso. The conformation of the lasso **5** was evidenced by comparing the NMR spectra of **5** with **4l** (Fig. 5b and c). In **5**, the chemical shifts of the hydrogen atoms $H_{13'}$ and $H_{15'}$, which belong to the ammonium station, are slightly affected by both the displacement of the DB24C8 and the introduction of the carbamoyl moiety. More importantly, significant variations are observed for the hydrogens of the triazolium site. Indeed, in **5**, the hydrogens H_{13} and H_{14} are both shifted downfield ($\Delta\delta = 0.2$ and 0.54 ppm, respectively) due to their interaction through hydrogen bonding with the oxygen atoms of the DB24C8. Furthermore, H_{14} appears split in the tightened lasso **5**, probably due to the more constrained asymmetric loop of the lasso. Meanwhile, H_{11}, H_{20} and in a lesser extent H_{10} are all shifted upfield in **5** ($\Delta\delta = -1.05$, -0.75 and -0.53 ppm, respectively), because they experience the shielding effect of the aromatic ring of the DB24C8. This is consistent with the fact that $H_{8'-11'}$ are all deshielded in **5**, because they no longer experience the shielding effect of the aromatic ring of the DB24C8. Besides, and for the same reason that H_{14}, H_{11} appear importantly split in **5**, this is an indicator of the constrained tightened lasso. The localization of the DB24C8 around the triazolium station could also be confirmed by direct comparison between the NMR spectra of **5** and **5u** (Fig. 5c and d). Briefly, the only differences of chemical shifts between **5** and **5u** concern the hydrogens of the DB24C8 and those of the triazolium station. As already mentioned, the hydrogens H_{C-H} of the crown ether are split in the interlocked architecture. Moreover, H_{13}, H_{14} and H_{15} are all shifted

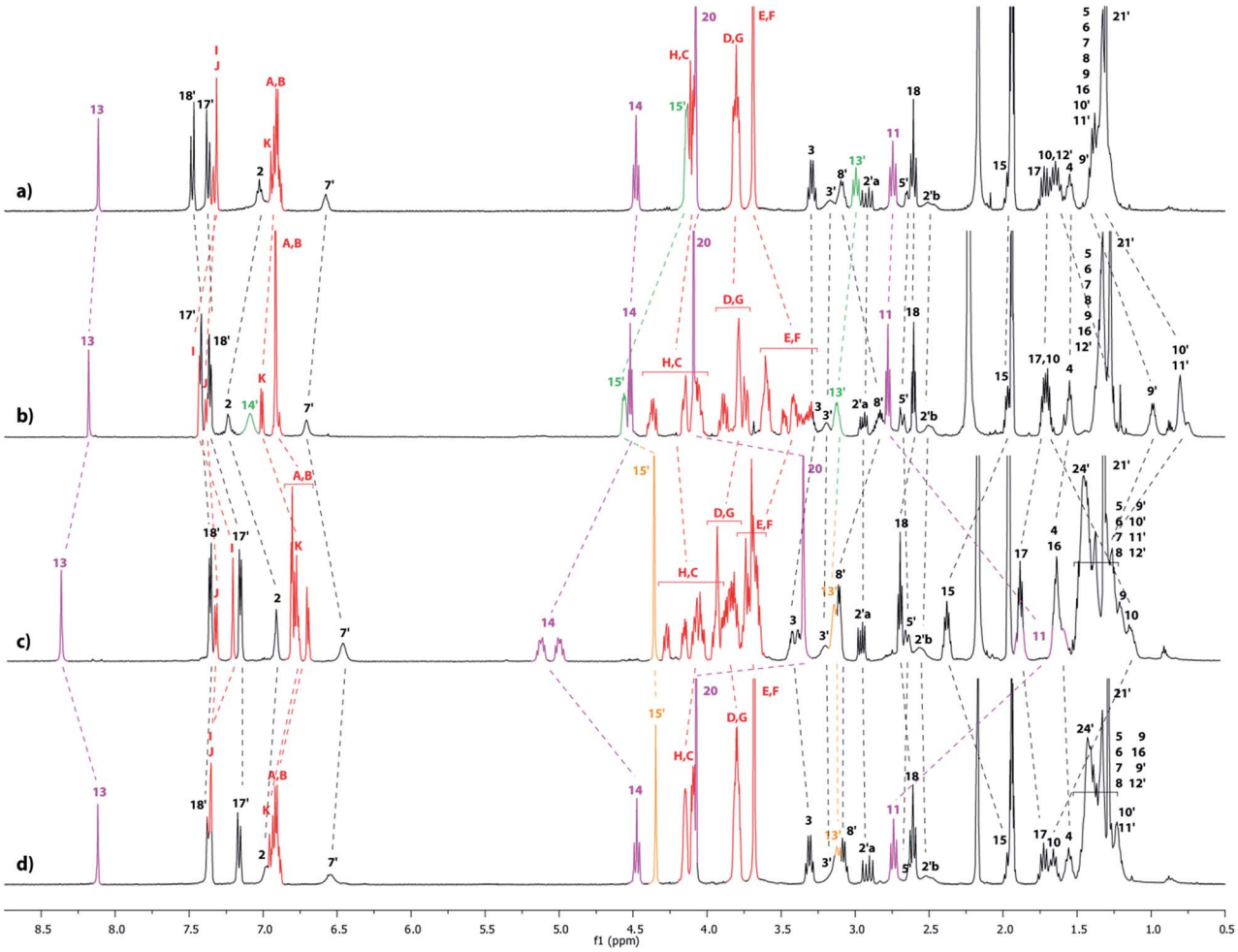

Fig. 5 ^{1}H NMR Spectra (600 MHz, CD_3CN, 298 K) of (a) the non-interlocked analogue **4u**, (b) the loosened [1]rotaxane **4l**, (c) the *N*-carbamoylated tightened [1]rotaxane **5** and (d) the non-interlocked analogue **5u**. The numbering and colorings correspond to the hydrogen assignments indicated in Scheme 1.

downfield in **5** ($\Delta\delta$ = +0.26, +0.59 and +0.41 ppm, respectively) with respect to **5u** due to their hydrogen-bonding interactions with the oxygen atoms of the crown ether. Finally, H_{11}, H_{20} and to a lesser extent H_{10}, are all shifted upfield in **5** ($\Delta\delta$ = −1.01, −0.73 and −0.48 ppm, respectively) because they are localized in the shielding cavity of the aromatic rings of the DB24C8.

Contraction of the tightened lasso 5 and characterization of the mono- and tris-branched triazolium-based [1]rotaxanes 6 and 7

The tightened lasso **5** was designed in such a fashion that the molecular surrounded axle contains a NHS ester that can be cleaved by an amino compound at the end of the multistep sequence. An amine and a triamine were separately added to **5** in order to synthesize the triazolium-based mono and the tris-branched [1]rotaxanes **6** and **7**, respectively (Scheme 1 and Fig. 2). Adding 2 equivalents of *tert*-butylbenzylamine in acetonitrile readily afforded the [1]rotaxane **6** in 87% yield after purification by Sephadex LH 20 chromatography. The synthesis of the tris-branched [1]rotaxane **7** was realized by adding a 0.3 equivalent of the 1,3,5-tris(aminomethyl)benzene to 1 equivalent of **5**. The reaction was not as efficient as for the synthesis of **6**, since only 13% of pure tris-branched [1]rotaxane **7** was isolated after successive Sephadex and silica gel chromatographies. In this case, the lower yield is not ascribed to a poorer conversion of the contraction reaction but rather to the very tricky purification of the final compound. Characterization of the interlocked molecular architectures **6** and **7** was realized by comparing their ^{1}H NMR spectra with those of their non-interlocked analogues **6u** and **7u** (Fig. 6 and 7, respectively).

In the [1]rotaxane **6** (with respect to **6u**), and like in all the DB24C8-based interlocked architectures, the methylene hydrogens H_{C-H} are all split because they are facing the two non-symmetrical ends of the threaded axle (Fig. 6). Besides, the hydrogens of the triazolium station are highly affected by the presence of the DB24C8. The hydrogen atoms H_{13} and H_{14} and H_{15} are shifted downfield in **6** ($\Delta\delta$ = 0.24, 0.58 and 0.39 ppm, respectively) because of their interactions through hydrogen bonding with the oxygen atoms of the crown ether. On the contrary, the hydrogens H_{10}, H_{11} and H_{20} are significantly

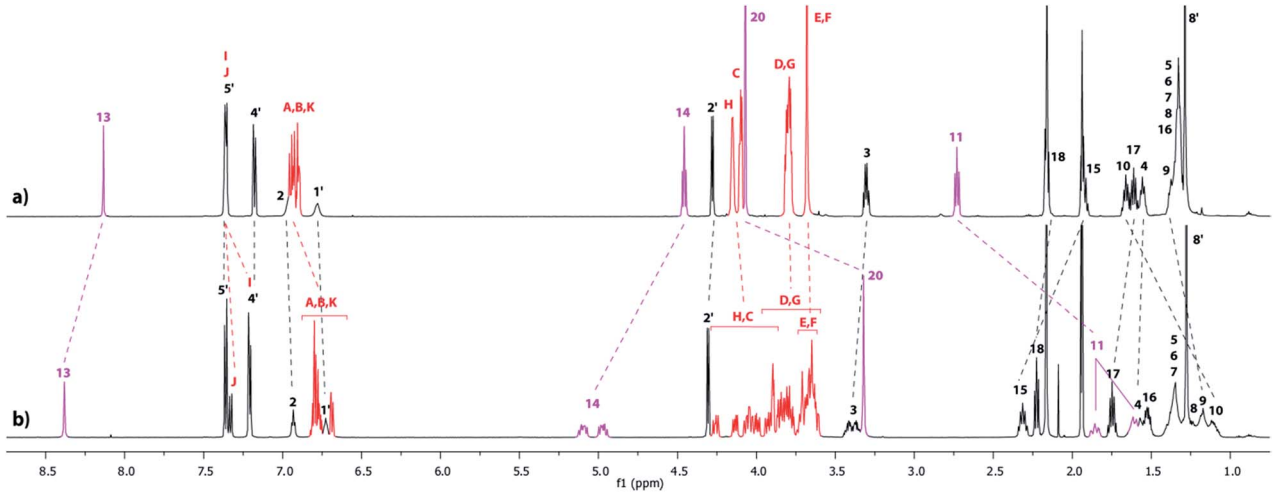

Fig. 6 ^{1}H NMR Spectra (600 MHz, CD_3CN, 298 K) of (a) the non-interlocked analogue **6u** and (b) triazolium-containing [1]rotaxane **6**. The numbering and colorings correspond to the hydrogen assignments indicated in Fig. 2.

shifted upfield ($\Delta\delta = -0.45$, -0.99 and -0.74 ppm, respectively) because they experience the shielding effect of the aromatic rings of the DB24C8. Of particular interest is the shape of the signals of the hydrogens that are in the loop of the lasso. Indeed, in the [1]rotaxane **6**, and as observed in the carbamoylated tightened lasso **5** (Fig. 5c) or in the protonated tightened lasso **4t** (Fig. 4c), the hydrogens H_{14}, H_{11}, and to a lesser extent H_3, all become split. The chirality of the reported [1]rotaxane architecture (*i.e.* left- or right-handed helix-type lasso), which is due to the non-symmetrical substitution of the crown ether by the threaded axle, may account for these results. In fact, the hydrogens that are localized in or close to the chiral loop become diastereotopic in the restrained tightened [1]rotaxane, and hence are split in the ^{1}H NMR spectrum. On contrary, no splitting of these hydrogens is observed in the non-interlocked compound **6u**, this being obvious due to the absence of the lasso.

Apart from the fact that the ^{1}H NMR spectrum of the tris-branched triazolium-containing [1]rotaxane **7** appears a little bit broader[21] than those of **6**, exactly the same trend concerning the chemical shift variations and the splitting of signals was observed between the [1]rotaxane **7** and its non-interlocked analogue **7u** (Fig. 7).

Conclusions

Even if interlocked components are considered as very attractive molecular targets, the efficient access to a wide range of them is still constrained, especially because they usually need to contain well-chosen moieties that can interact together in order to drive their assembly. In this paper, we have reported the efficient and straightforward preparation of triazolium-containing mono- or tris-branched [1]rotaxanes that could not be obtained through classical methods. Whereas triazolium

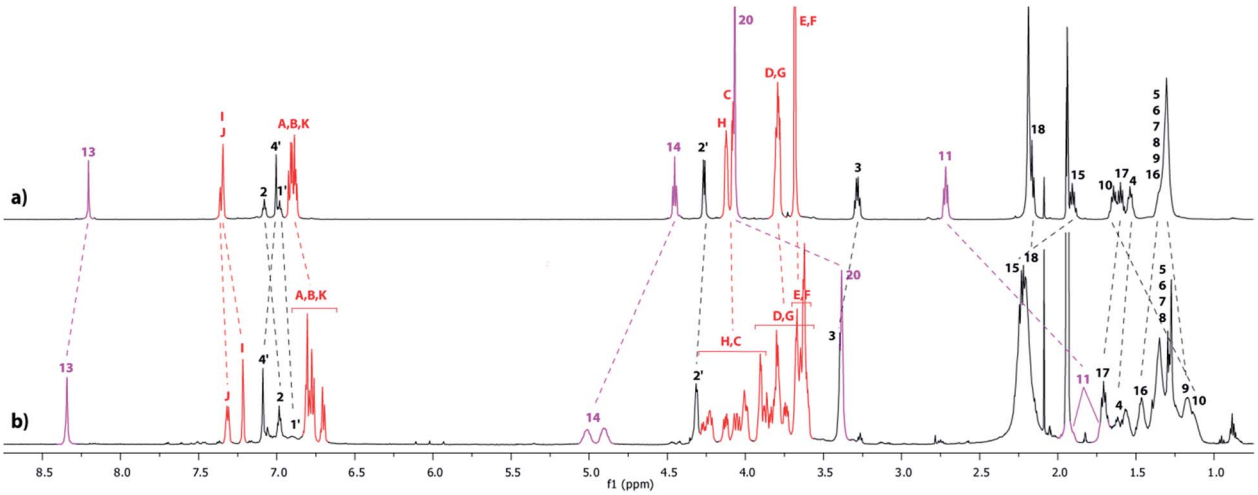

Fig. 7 ^{1}H NMR Spectra (600 MHz, CD_3CN, 298 K) of (a) the non-interlocked analogue **7u** and (b) triazolium-containing [1]rotaxane **7**. The numbering and colorings correspond to the hydrogen assignments indicated in Fig. 2.

consists of a quite effective molecular station for DB24C8 derivatives in a locked structure like rotaxane, it cannot be used as a template to drive the formation of a DB24C8-based interlocked component through intermolecular interactions. This is mainly due to the too weak interactions between the moieties. The possibility to hypothetically synthesize a triazolium-based semirotaxane, from a DB24C8 derivative and a triazolium-containing molecular axle, is highly limited by the loss in entropic factor, which becomes here predominant with respect to the weak gain in enthalpy (*i.e.* the very weak interactions between the two components). Here, the triazolium-containing [1]rotaxane **6** could be obtained using a five-step sequence from the azidohexanoic acid in a 36% overall yield. The possibility to add a polyamine at the last step of the synthesis allows extension of the method to multi-branched[22] triazolium-based [1]rotaxanes. As an example, the tris-branched [1]rotaxane **7** was prepared and isolated. The improvement of the chemical access to a wide range of [1]rotaxanes that does not necessarily contain a template is a substantial advance for the synthesis of new structures of interest.

Acknowledgements

P. W. is funded by the LABEX ChemiSyst (ANR-10-LABX-05-01).

Notes and references

1 (*a*) S. F. M. van Dongen, S. Cantekin, J. A. A. W. Elemans, A. E. Rowan and R. J. M. Nolte, *Chem. Soc. Rev.*, 2014, **43**, 99–122; (*b*) M. S. Vickers and P. D. Beer, *Chem. Soc. Rev.*, 2007, **36**, 211–225; (*c*) E. R. Kay, D. A. Leigh and F. Zerbetto, *Angew. Chem., Int. Ed.*, 2007, **46**, 72–191; (*d*) J. F. Stoddart, *Angew. Chem., Int. Ed.*, 2014, **53**, 11102–11104; (*e*) J.-P. Sauvage, C. Dietrich-Buchecker and G. Rapenne, in *Molecular Catenanes, Rotaxanes and Knots*, ed. J.-P. Sauvage and C. Dietrich-Buchecker, Wiley-VCH Weinheim, 1999, ch. 6, pp. 107–139; (*f*) G. A. Breault, C. A. Hunter and P. C. Mayers, *Tetrahedron*, 1999, **55**, 5265–5293; (*g*) G. Barin, A. Coskun, M. M. G. Fouda and J. F. Stoddart, *ChemPlusChem*, 2012, **77**, 159–185; (*h*) B. Champin, P. Mobian and J.-P. Sauvage, *Chem. Soc. Rev.*, 2007, **36**, 358–366; (*i*) J. F. Stoddart, *Chem. Soc. Rev.*, 2009, **38**, 1802–1820; (*j*) J.-P. Sauvage, *Acc. Chem. Res.*, 1998, **31**, 611–619; (*k*) D. H. Qu and H. Tian, *Chem. Sci.*, 2011, **2**, 1011–1015; (*l*) D.-H. Qu, Q.-C. Wang, Q.-W. Zhang, X. Ma and H. Tian, *Chem. Rev.*, 2015, DOI: 10.1021/cr5006342.

2 F. Coutrot, in *Advances in Atom and Single Molecule Machines, Single Molecular Machines and Motors*, ed. C. Joachim and G. Rapenne, Springer International Publishing, Switzerland, 2015, p. 35.

3 K. Hiratani, M. Kaneyama, Y. Nagawa, E. Koyama and M. Kanesato, *J. Am. Chem. Soc.*, 2004, **126**, 13568–13569.

4 (*a*) P. Franchi, P. Fani, E. Mezzina and M. Lucarini, *Org. Lett.*, 2008, **10**, 1901–1904; (*b*) Q. Zhou, P. Wei, Y. Zhang, Y. Yu and X. Yan, *Org. Lett.*, 2013, **15**, 5350–5353.

5 (*a*) X. Ma, Q. Wang and H. Tian, *Tetrahedron Lett.*, 2007, **48**, 7112–7116; (*b*) L. Zhu, H. Yan and Y. Zhao, *Int. J. Mol. Sci.*, 2012, **13**, 10132–10142; (*c*) H. Li, J.-N. Zhang, W. Zhou, H. Zhang, Q. Zhang, D.-H. Qu and H. Tian, *Org. Lett.*, 2013, **15**, 3070–3073; (*d*) H. Li, X. Li, H. Agren and D.-H. Qu, *Org. Lett.*, 2014, **16**, 4940–4943; (*e*) X. Ma, D.-H. Qu, F. Ji, Q. Wang, L. Zhu, Y. Xu and H. Tian, *Chem. Commun.*, 2007, 1409–1411; (*f*) H. Li, H. Zhang, Q. Zhang, Q.-W. Zhang and D. Qu, *Org. Lett.*, 2012, **14**, 5900–5903.

6 S. Tsuda, J. Terao and N. Kambe, *Chem. Lett.*, 2009, **38**, 76–77.

7 (*a*) Z. Xue and M. F. Mayer, *J. Am. Chem. Soc.*, 2010, **132**, 3274–3276; (*b*) C. Clavel, C. Romuald, E. Brabet and F. Coutrot, *Chem.–Eur. J.*, 2013, **19**, 2982–2989; (*c*) C. Clavel, K. Fournel-Marotte and F. Coutrot, *Molecules*, 2013, **18**, 11553–11575.

8 S. Chao, C. Romuald, K. Fournel-Marotte, C. Clavel and F. Coutrot, *Angew. Chem., Int. Ed.*, 2014, **53**, 6914–6919.

9 Apart from ref. 8, only one other similar approach has been reported to date, however for the preparation of [2]rotaxanes using a five-component "clipping" rotaxane formation, see: J. S. Hannam, S. M. Lacy, D. A. Leigh, C. G. Saiz, A. M. Z. Slawin and S. G. Stitchell, *Angew. Chem., Int. Ed.*, 2004, **43**, 3260–3264.

10 (*a*) P. R. Ashton, I. Baxter, M. C. T. Fyfe, F. M. Raymo, N. Spencer, J. F. Stoddart, A. J. P. White and D. J. Williams, *J. Am. Chem. Soc.*, 1998, **120**, 2297–2307; (*b*) Y. Tokunaga, N. Wakamatsu, A. Ohbayashi, K. Akasaka, S. Saeki, T. Hisada, T. Goda and Y. Shimomura, *Tetrahedron Lett.*, 2006, **47**, 2679–2682; (*c*) F. M. Raymo, K. N. Houk and J. F. Stoddart, *J. Am. Chem. Soc.*, 1998, **120**, 9318–9322; (*d*) F. M. Raymo and J. F. Stoddart, *Pure Appl. Chem.*, 1997, **69**, 1987–1997; (*e*) M. Händel, M. Plevoets, S. Gestermann and F. Vögtle, *Angew. Chem., Int. Ed. Engl.*, 1997, **36**, 1199–1201; (*f*) S.-Y. Hsueh, C.-C. Lai, Y.-H. Liu, Y. Wang, S.-M. Peng and C.-C. Hsu, *Org. Lett.*, 2007, **9**, 4523–4526; (*g*) J.-J. Lee, A. G. White, J. M. Baumes and B. D. Smith, *Chem. Commun.*, 2010, **46**, 1068–1069; (*h*) A. J. McConnell and P. D. Beer, *Chem.–Eur. J.*, 2011, **17**, 2724–2733; (*i*) P. R. Ashton, M. Belohradsky, D. Philp and J. F. Stoddart, *J. Chem. Soc., Chem. Commun.*, 1993, 1269–1274; (*j*) M. Asakawa, P. R. Ashton, R. Ballardini, V. Balzani, M. Belohradsky, M. T. Gandolfi, O. Kocian, L. Prodi, F. M. Raymo, J. F. Stoddart and M. Venturi, *J. Am. Chem. Soc.*, 1997, **119**, 302–310; (*k*) M. A. Bolla, J. Tiburcio and S. J. Loeb, *Tetrahedron*, 2008, **64**, 8423–8427; (*l*) P. Linnartz, S. Bitter and C. A. Schalley, *Eur. J. Org. Chem.*, 2003, 4819–4829; (*m*) H. W. Gibson, N. Yamaguchi, Z. Niu, J. W. Jones, C. Slebodnick, A. L. Rheingold, L. N. Zakharov and J. Polym, *J. Polym. Sci., Part A: Polym. Chem.*, 2010, **48**, 975–985.

11 A. G. Kolchinski, D. H. Busch and N. W. Alcock, *J. Chem. Soc., Chem. Commun.*, 1995, 1289–1291.

12 (*a*) R. Huisgen, *Pure Appl. Chem.*, 1989, **61**, 613–628; (*b*) R. Huisgen, G. Szeimies and L. Möbius, *Chem. Ber.*, 1967, **100**, 2494–2507; (*c*) R. Huisgen, *Angew. Chem.*, 1963, **75**, 604–637; *Angew. Chem., Int. Ed. Engl.*, 1963, **2**, 565–598; (*d*) R. Huisgen, *Angew. Chem.*, 1963, **75**, 742–754; *Angew. Chem., Int. Ed. Engl.*, 1963, **2**, 633–645.

13 (*a*) H. C. Kolb, M. G. Finn and K. B. Sharpless, *Angew. Chem., Int. Ed.*, 2001, **40**, 2004–2021; (*b*) C. W. Tornoe,

C. Christensen and M. Meldal, *J. Org. Chem.*, 2002, **67**, 3057–3064.

14 (*a*) F. Coutrot and E. Busseron, *Chem.–Eur. J.*, 2008, **14**, 4784–4787; (*b*) F. Coutrot, C. Romuald and E. Busseron, *Org. Lett.*, 2008, **10**(17), 3741–3744; (*c*) F. Coutrot, *ChemistryOpen*, DOI: 10.1002/open.201500088.

15 The shuttling of the macrocycle between the two stations is slow at the NMR timescale.

16 Exactly the same trend of variations of the chemical shifts between hydrogens of **4l** and **4u** is observed in DMSO-d_6 at $t = 0$ and in CD_3CN, corroborating the localization of the DB24C8 around the ammonium station in both solvents.

17 For **4t** in DMSO, it is interesting to note that H_{13} is unusually shielded by the aromatic rings of the crown ether, instead of being shifted downfield due to hydrogen-bonding interactions. This is ascribed to two concomitant factors. First, the high polarity of the DMSO solvent decreases the strength of hydrogen bonds. Second, the constrained tightened lasso structure does not allow an optimal tridimensional arrangement between H_{13} and the oxygen atoms of the crown ether without inducing steric repulsion. Therefore, in this particular case, the oxygen atoms of the crown ether prefer to interact through hydrogen bonds with the sole hydrogen atoms H_{14} which are located slightly further from the loop. A similar shielding effect underwent by the considered triazolium hydrogen was noticed once in a tightened BMP25C8-based [1]rotaxane. In that case, the larger crown ether (not the solvent) and the constrained lasso both disfavour the hydrogen bond between the triazolium hydrogen and the oxygen atoms of the BMP25C8, resulting in the same shielding effect, even in the less polar dichloromethane, see ref. 7*b*.

18 Y. Tachibana, H. Kawasaki, N. Kihara and T. Takata, *J. Org. Chem.*, 2006, **71**, 5093–5104.

19 C. Romuald, E. Busseron and F. Coutrot, *J. Org. Chem.*, 2010, **75**, 6516–6531.

20 The [1]rotaxanes **5**, **4** and **3**, as well as the [2]rotaxane **2**, may exist as a mixture of stereoisomers which are not distinguishable by ^{1}H NMR. They arise from both the (*R*)/(*S*) stereochemistry of the asymmetric carbon of the NHS moiety and the non-symmetrical substitution of the DB24C8. For recent examples about stereoisomerism in rotaxane structures, see: (*a*) C. Reuter, C. Seel, M. Nieger and F. Vögtle, *Helv. Chim. Acta*, 2000, **83**, 630–640; (*b*) Q.-F. Luo, L. Zhu, S.-J. Rao, H. Li, Q. Miao and D.-H. Qu, *J. Org. Chem.*, 2015, **80**, 4704–4709; (*c*) R. J. Bordoli and S. M. Goldup, *J. Am. Chem. Soc.*, 2014, **136**, 4817–4820.

21 The broadness of the ^{1}H NMR spectrum of **7** may result from the existence of several stereoisomers, due to the chiral loop of the lasso (*i.e.* right- or left-handed helix type lasso).

22 For recent multi-branched interlocked structures, see: (*a*) J.-N. Zhang, H. Li, W. Zhou, S.-L. Yu, D.-H. Qu and H. Tian, *Chem.–Eur. J.*, 2013, **19**, 17192–17200; (*b*) H. Zhang, Q. Liu, J. Li and D.-H. Qu, *Org. Lett.*, 2013, **15**, 338–341; (*c*) H. Li, X. Li, Z.-Q. Cao, D.-H. Qu, H. Ågren and H. Tian, *ACS Appl. Mater. Interfaces*, 2014, **6**, 18921–18929.